Numerical study on aerodynamic damping of floating vertical axis wind turbines

Numerical study on aerodynamic damping of floating vertical axis wind turbines

Zhengshun Cheng[1,2,3]**, Helge Aagaard Madsen**[4]**, Zhen Gao**[1,2,3] **and Torgeir Moan**[1,2,3]

[1] Department of Marine Technology, Norwegian University of Science and Technology (NTNU), Trondheim, NO-7491, Norway
[2] Centre for Ships and Ocean Structures (CeSOS), NTNU, Trondheim, NO-7491, Norway
[3] Centre for Autonomous Marine Operations and Systems (AMOS), NTNU, Trondheim, NO-7491, Norway
[4] Department of Wind Energy, Technical University of Denmark, Roskilde, 4000, Denmark

E-mail: `zhengshun.cheng@ntnu.no`

Abstract. Harvesting offshore wind energy resources using floating vertical axis wind turbines (VAWTs) has attracted an increasing interest in recent years. Due to its potential impact on fatigue damage, the aerodynamic damping should be considered in the preliminary design of a floating VAWT based on the frequency domain method. However, currently the study on aerodynamic damping of floating VAWTs is very limited. Due to the essential difference in aerodynamic load characteristics, the aerodynamic damping of a floating VAWT could be different from that of a floating horizontal axis wind turbine (HAWT). In this study, the aerodynamic damping of floating VAWTs was studied in a fully coupled manner, and its influential factors and its effects on the motions, especially the pitch motion, were demonstrated. Three straight-bladed floating VAWTs with identical solidity and with a blade number varying from two to four were considered. The aerodynamic damping under steady and turbulent wind conditions were estimated using fully coupled aero-hydro-servo-elastic time domain simulations. It is found that the aerodynamic damping ratio of the considered floating VAWTs ranges from 1.8% to 5.3%. Moreover, the aerodynamic damping is almost independent of the rotor azimuth angle, and is to some extent sensitive to the blade number.

1. Introduction

Aerodynamic damping plays an important role in the design of support structure for offshore wind turbines, since it can reduce fatigue significantly [1]. Previous study on aerodynamic damping is mainly carried out for offshore horizontal axis wind turbines (HAWTs), which is now dominating the offshore wind energy market. For HAWTs, the aerodynamic damping is related to the variation in thrust caused by a variation in the axial wind speed [1].

Floating vertical axis wind turbine is also considered as a very promising alternative to harvest wind energy resource in deep water, since it provides a potential of cost of energy reduction [2]. Compared with a floating HAWT, the aerodynamic loads of a floating VAWT vary periodically and significantly [3]. In particular, the variation in thrust is a result of a variation in axial wind speed as well as in rotor azimuth angle. The latter one is especially relevant for a two-bladed VAWT, since its thrust can vary from almost zero to approximately double the mean value during

one rotation. Therefore, the aerodynamic damping resulting from these varying aerodynamic loads for a floating VAWT is to some extent different from that of a floating HAWT.

To date very limited study on the aerodynamic damping of floating VAWTs has been carried out. Antonutti [4] conducted a preliminary study on the effect of aerodynamic damping on the pitch motion of a floating VAWT using time domain simulations. The floating VAWT considered was the DeepWind 5MW Darrieus rotor with a semi-submersible floater. However, the controller dynamics and structural dynamics were ignored and the mooring system was simplified based on a force-displacement relationship. Therefore, a more comprehensive study on aerodynamic damping using a fully coupled aero-hydro-servo-elastic method is of great interest for floating VAWTs. Moreover, the estimation approach and influential factor of the aerodynamic damping, and its potential effect on the dynamic behavior of a floating VAWT are not throughly studied yet.

In this study the aerodynamic damping effect on the motions of floating VAWTs was numerically estimated and addressed. Three VAWTs with straight and parallel blades, with identical solidity and with a blade number varying from two to four was mounted on a semi-submersible. A series of time domain simulations were carried out using a fully coupled aero-hydro-servo-elastic simulation tool SIMO-RIFLEX-AC [5]. In this way, the contribution to the variation in the thrust from a variation in wind speed and from a change in rotor azimuth angle was both considered. In addition, the effect of the number of blades on the aerodynamic damping level was also demonstrated.

2. Description of floating VAWT models

In this study, three floating VAWTs mounted on a semi-submersible [6] were considered, as depicted in Figure 1. The three rotors consist of parallel straight blades and hold the same solidity while the number of blades varies from two to four. Specifications of these three rotors are given in Table 1. The semi-submersible used was obtained on the basis of the OC4 semi-submersible [7], which was originally designed to support the NREL 5 MW wind turbine [8]. Due to the difference in the rotor mass between the present VAWTs and the NREL 5 MW

(a) Straight-bladed Semi-submersible VAWTs   (b) Top view of the blades
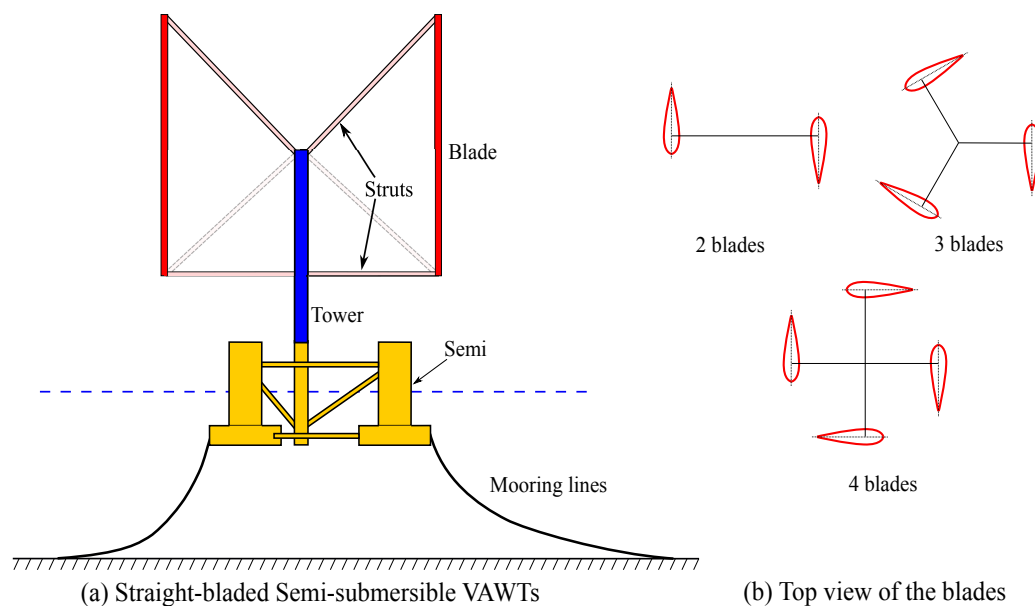
Figure 1. Floating VAWTs with straight and parallel blades and with a blade number ranging from two to four.

wind turbine, the ballast of the semi-submersible was adjusted to maintain the same draft and displacement. Properties of the three floating VAWT systems are given in Table 1. More details about the floating VAWT systems, such as specifications of the rotors and structural and hydrodynamic properties of the systems, are described by Cheng et al. [6].

Table 1. Properties of the three floating VAWT systems. [6]

	Semi H2	Semi H3	Semi H4
Blade number [-]	2	3	4
Rotor radius [m]	39.0	39.0	39.0
Blade height [m]	80.0	80.0	80.0
Chord length [m]	4.05	2.7	2.03
Water depth [m]	200	200	200
Draft [m]	20	20	20
Diameter at mean water line [m]	12.0/6.5	12.0/6.5	12.0/6.5
Rotor mass [ton]	350.1	315.3	287.7
Center of mass for rotor [m]	(0, 0, 51.03)	(0, 0, 48.14)	(0, 0, 45.34)
Platform mass, including ballast and generator [ton]	13761.3	13796.1	13823.7
Center of mass for platform [m]	(0, 0, -13.44)	(0, 0, -13.43)	(0, 0, -13.43)
Buoyancy in undisplaced position [kN]	139816	139816	139816
Center of buoyancy [m]	(0, 0, -13.15)	(0, 0, -13.15)	(0, 0, -13.15)
Surge/Sway [s]	113.15	113.15	113.15
Heave [s]	17.04	17.04	17.04
Pitch/Roll [s]	21.17	20.68	20.32
Yaw [s]	80.38	80.44	80.49

(a) Generator power
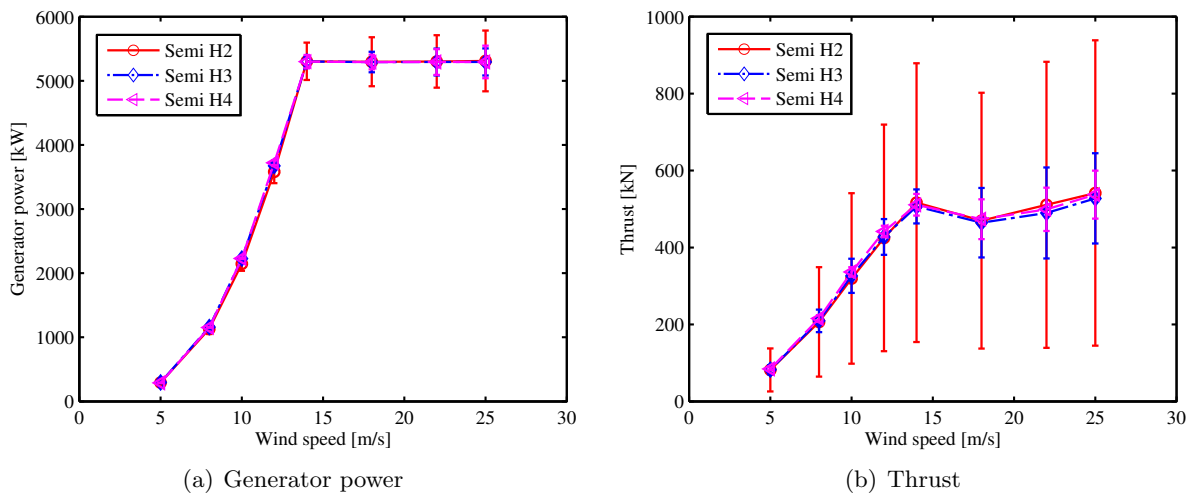
(b) Thrust

Figure 2. The mean value and standard deviation of generator power and thrust of the three floating VAWTs steady wind conditions. The "error bar" indicates the standard deviation.

3. Fully coupled numerical method

The fully coupled code SIMO-RIFLEX-AC, developed by Cheng et al. [5], is used to carry out the integrated dynamic analysis of floating VAWTs. The SIMO [9] and RIFLEX [10] codes were developed by MARINTEK and have been widely used in the offshore oil and gas industry. The SIMO-RIFLEX-AC code is capable of accounting for the turbulent wind inflow, aerodynamics, hydrodynamics, structural dynamics, control system dynamics and mooring line dynamics. It

integrates three computer codes: SIMO [9] computes the hydrodynamic loads acting on the platform hull based on a combination of the potential flow theory and Morison's equation; RIFLEX [10] models the blades, tower, shaft, struts and mooring lines using flexible finite elements and provides links to an external controller and AC; and AC calculates the aerodynamic loads acting on the blades based on the Actuator Cylinder flow method. Moreover, a generator torque controller based on a proportional-integral (PI) algorithm is implemented to regulate the rotor rotational speed.

The AC method, which is originally developed by Madsen [11] and further discussed and detailed by Cheng et al. [12], is a 2D quasi-steady flow model. It extends the actuator disc concept to an actuator surface coinciding with the swept area of the 2D VAWT. Based on the continuity equation and Euler equation, the induced velocities are thus related to the volume forces, which can be determined from the normal and tangential forces resulting from the blade forces. The induced velocity includes a linear part and a nonlinear part; the linear part can be computed analytically. However, it's to some extent time-consuming to compute the nonlinear solution directly. A modified linear solution is therefore proposed to approximate the final solution.

The induced velocities calculated are based on a steady state equilibrium without time. To account for the dynamic inflow effect, a low pass filter proposed by Larsen and Madsen [13] is applied on the calculated steady-state induced velocities. This is parallel to how dynamic inflow effects are taken into account in the blade element momentum (BEM) theory for HAWTs. The same non-dimensional filter constants as for the HAWTs are used and they are then scaled proportionally with the diameter of the VAWT and inversely with the wind speed. It should be noted that this dynamic inflow model is not yet validated for VAWTs due to the limited experimental data. The AC model implemented in [5] also includes the effects of wind shear and turbulence, and dynamic stall. The effect of dynamic stall is incorporated using the Beddoes-Leishman model. The aerodynamic model AC has been validated with experiment results [12] and the SIMO-RIFLEX-AC code has been verified by a series of numerical comparisons with other computer codes [5].

4. Approach for aerodynamic damping estimation

The analysis of free decay in pitch motion is a simple and straight forward method to estimate the aerodynamic damping of a floating wind turbine. Nonlinear time domain simulations are usually conducted, in which a moment is slowly applied at the mean water level until the floating turbine reaches a static equilibrium. The moment is released afterwards and the pitch motion is recorded. In this way, the system damping ratio can be calculated as follows

$$\xi_{system} = \frac{\delta}{\sqrt{4\pi^2 + \delta^2}} \qquad (1)$$

where the logarithmic decrement δ is defined in terms of the ith and $(m+i)^{th}$ peak of pitch motion as

$$\delta = \frac{1}{m} \log\left(\frac{x_i}{x_{m+i}}\right) \qquad (2)$$

The system damping ratio calculated in Eq. 1 is usually a combination of damping ratios from different sources, such as water, air, and structures. Given other damping ratios such as structural and hydrodynamic damping, the aerodynamic damping can thus be computed as

$$\xi_{aero} = \xi_{system} - \xi_{other} \qquad (3)$$

The above approach applies well for a floating HAWT, since its thrust force has a very small variation at a given wind speed, which can cause a smooth pitch motion with negligible high-frequency variation. However, this approach can not be directly used for a floating VAWT,

since the pitch motion, especially of a two-bladed floating VAWT, usually consists of a low-frequency component as well as a visible high-frequency component. And the high-frequency component is related to the periodic variation of thrust force. In order to use this approach for the aerodynamic damping estimation, the low- and high-frequency component can be handled separately by using, for instance, a band-pass filter.

5. Results and discussions

In this study, the decay in pitch motion under calm water, under steady wind and under turbulent wind was considered for each floating VAWT. The free decay in calm water was used to estimate the damping ratios from structure and water, which correspond to the term ξ_{other} in Eq. 3. The rotors are assumed to be parked and the effect of different rotor azimuth angle when parked on the damping ratio is neglected. The time history of pitch decay of the three floating VAWTs in calm water is demonstrated in Figure 3. The damping ratio resulting from hydrodynamic damping and structural damping is found to be very close to each other. Analyzing using the aforementioned approach gives a damping ratio of 1.72% for each floating VAWTs.
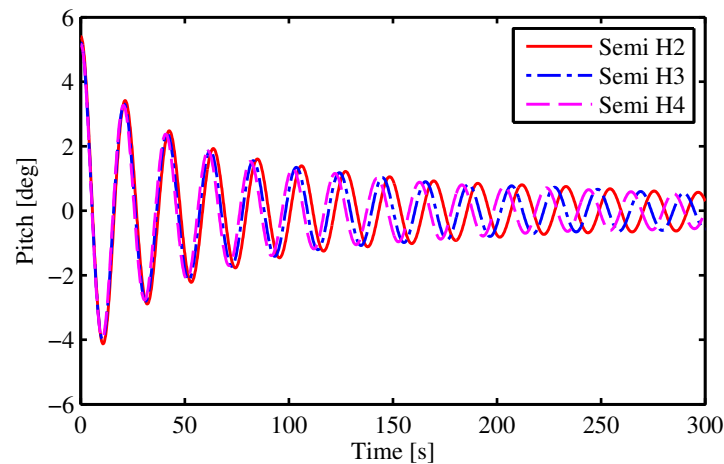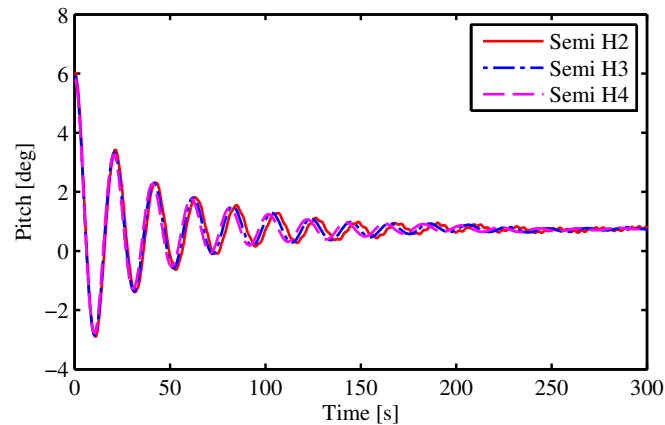

Figure 3. Free decay of pitch motion for the three floating VAWTs in calm water.

For the steady and turbulent wind conditions, the system damping ratio and aerodynamic damping are estimated under normal operating conditions. A generator torque controller based on a PID control algorithm, as described by Cheng et al. [6], is used to regulate the rotor rotational speed. Eight representative wind speeds ranging from 5 m/s to 25 m/s are considered, respectively. Fully coupled time domain simulations were carried out using the SIMO-RIFLEX-AC code. The aerodynamic damping under steady and turbulent winds is then estimated using the aforementioned method.

5.1. Aerodynamic damping under steady wind

Figure 4 shows the time history of pitch decay of the three floating VAWTs under steady wind conditions, with a wind speed of 8 and 18 m/s, respectively. It can be observed that the pitch motion decays at U_w=8 m/s much faster than that at U_w=18 m/s, indicating a higher system damping as well as an higher aerodynamic damping at wind speed U_w=8 m/s.

Moreover, different frequency components that contribute to the decay time history in steady wind conditions are also illustrated in Figure 4. For the 3- and 4-bladed floating VAWTs, only a low-frequency component is observed, while not only a low-frequency component but also a very small high-frequency one are observed for the 2-bladed floating VAWT, as the close up shown

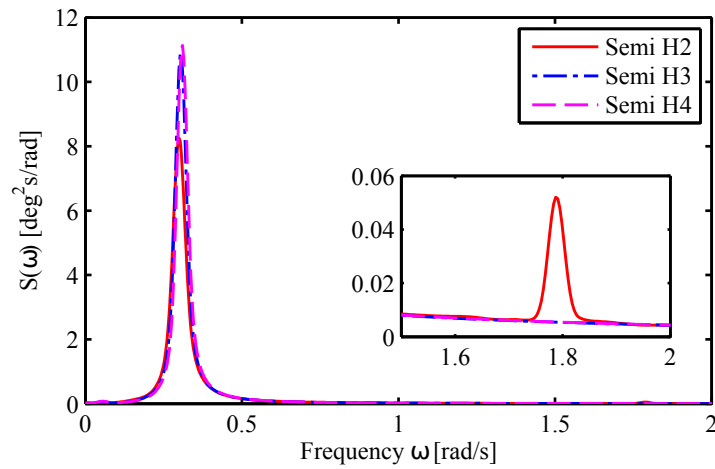(a) Pitch decay in steady wind U_w=8 m/s
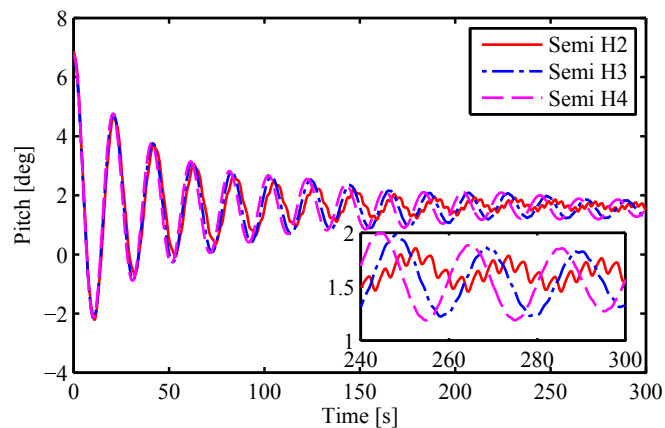
(b) Pitch decay in steady wind U_w=18 m/s

Figure 4. Decay of pitch motion for the three floating VAWTs under steady wind only conditions.

in Figure 4(b). This can also be revealed by conducting power spectral analysis, as shown in Figure 5. It can be found that the pitch resonant response is extremely dominating for these three floating VAWTs. A very tiny 2P response is observed only for the 2-bladed floating VAWT, while no 3P or 4P responses are observed for the 3- and 4-bladed floating VAWTs.

Using a band-pass filter, the low-frequency component and high-frequency component are illustrated in Figure 6. The high-frequency component is mainly due to the periodically varying aerodynamic loads, which are related to different rotor azimuth angle. When the rotor rotates, the azimuth angle of each blade varies. The aerodynamic lift and drag acting on each blade of the 2-bladed turbine can reach the maximum at the same azimuth angle, resulting a relatively larger fluctuation in resultant aerodynamic loads. While for the 3- and 4-bladed turbines, the aerodynamic lift and drag on each blade can to some extent cancel with each other, which causes a relatively smaller variation. However, due to the compliant catenary mooring system, the impact of rotor azimuth angle on platform motions is very small for the 2-, 3- and 4-bladed turbines, as demonstrated in Figure 6. As a result, the effect of rotor azimuth angle on the aerodynamic damping is very small as well.
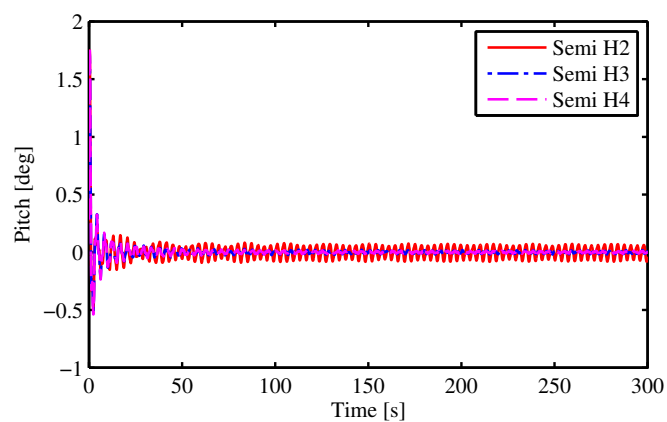
The low-frequency component of the time-history is then used to estimate the system damping ratio as well as the aerodynamic damping based on the method described in Section 4. The

Figure 5. Power spectral analysis of pitch decay of the three floating VAWTs under steady wind with U_w=18 m/s.
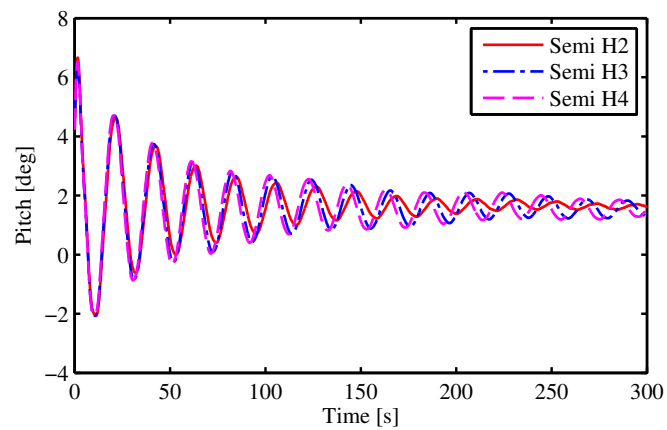

(a) Low frequency component

(b) High frequency component

Figure 6. Decay of pitch motion for the three floating VAWTs under steady wind only condition with a wind speed of 18 m/s.

aerodynamic damping for these three floating VAWTs are demonstrated in Figure 7. During the normal operating condition, the aerodynamic damping ranges from 1.8% to 5.3% for the three floating VAWTs. At the optimal tip speed ratio (TSR) region, the aerodynamic damping increases as wind speed increases for the three floating VAWTs. At the moderate TSR region, the aerodynamic holds at a relatively high level despite the increase of wind speed. However, there is a drop in the aerodynamic damping at wind speed of 18 m/s in the low TSR region, since there is a dramatic drop in the rotor rotational speed to maintain a constant mean generator power production, causing a decrease in the thrust. At higher wind speed, the aerodynamic damping returns to a relatively large level.

In addition, the effect of blade number on the aerodynamic damping is also demonstrated in Figure 7. At the optimal and moderate TSR regions, the three floating VAWTs have relatively close aerodynamic damping, indicating that the effect of blade number is relatively small. However, in the low TSR region, the aerodynamic damping of 3- and 4-bladed floating VAWTs are still relatively close, while that of the 2-bladed floating VAWT is much larger. The possible reason is that the dynamic stall effects on the 2-bladed floating VAWT is much stronger. Therefore, increasing the blade number from 3 to 4 does not affect the aerodynamic damping, but increasing the blade number from 2 to 3 will decrease the aerodynamic damping level, especially at the low TSR region.
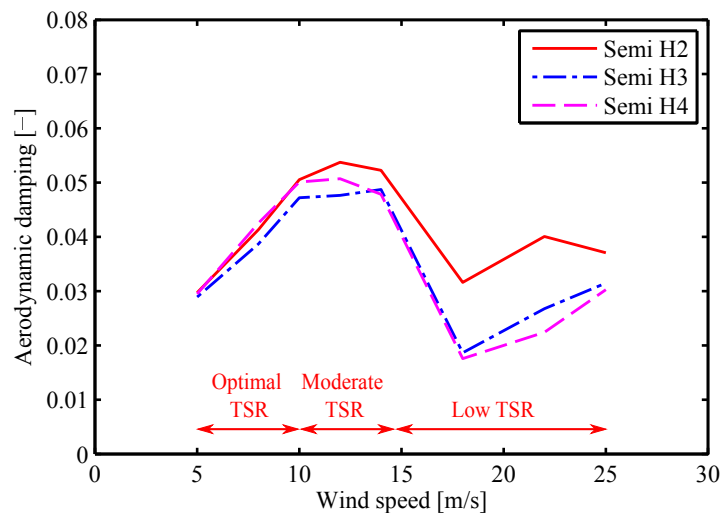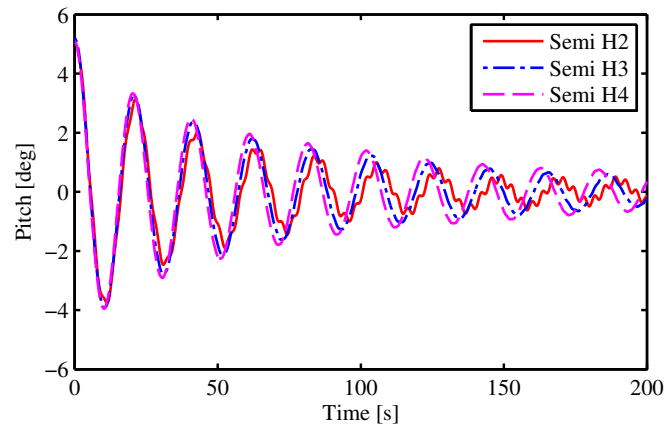

Figure 7. Aerodynamic damping of the three floating VAWTs under steady wind.

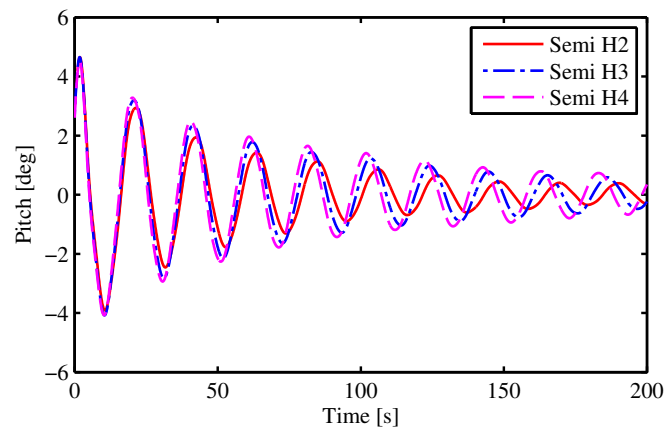### 5.2. Aerodynamic damping under turbulent wind

Aerodynamic damping was also estimated under turbulent wind conditions. Simulations with and without an external moment were conducted under the same turbulent wind field. The pitch decay caused by the external moment is then obtained by subtracting the pitch motions. Eight representative wind speeds and five seeds for each wind speed were considered.

An example of the pitch decay time history of the three floating VAWTs under turbulent wind is shown in Figure 8(a). As observed in the steady wind conditions, a very small high-frequency component is only visible for the 2-bladed floating VAWT. Hence the low-frequency component, as shown in Figure 8(b), is used to estimate the system damping as well as the aerodynamic damping.

The aerodynamic damping under turbulent wind conditions is illustrated in Figure 9. Each dot represents an aerodynamic damping estimated from one time domain simulation. Generally
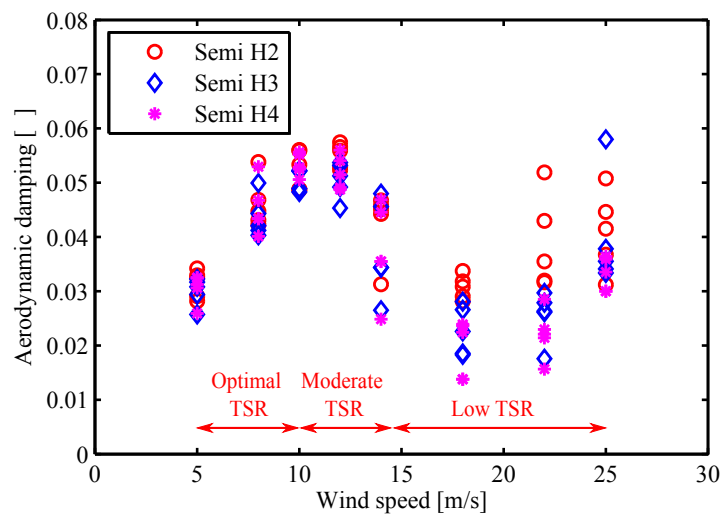
(a) Decay time history

(b) Low frequency component

Figure 8. Decay of pitch motion for the three floating VAWTs under turbulent wind only condition with a mean wind speed of 18 m/s.

Figure 9. Aerodynamic damping of the three floating VAWTs under turbulent wind.

speaking, the aerodynamic damping under turbulent wind conditions follows the same trend as that under steady wind conditions. Moreover, the aerodynamic damping estimated at a relatively high tip speed ratio is more concentrated than that at a relatively low tip speed ratio.

6. Conclusions

In this paper, the aerodynamic damping effect on the motions of floating vertical axis wind turbines (VAWTs) were numerical studied in a fully coupled way. And the level of aerodynamic damping and its influential factors were demonstrated. Three floating VAWTs with straight and parallel blades, with identical solidity and with a blade number ranging from two to four were considered. Fully coupled time domain simulations under steady and turbulent wind conditions were conducted using the code SIMO-RIFLEX-AC.

The aerodynamic damping of the floating VAWTs considered ranges from 1.8% to 5.3%. The rotor azimuth angle can cause periodical variations in the aerodynamic loads of a floating VAWT, but its impact on the aerodynamic damping is negligible.

The aerodynamic damping level of floating VAWTs is to some extent dependent on the blade number. By increasing the blade number from 3 to 4 does not affect the aerodynamic damping; however, increasing the blade number from 2 to 3 will decrease the aerodynamic damping level, especially at the low tip speed ratio region.

The aerodynamic damping estimated under steady wind conditions and turbulent wind conditions presents similar trend. Moreover, the aerodynamic damping under turbulent wind conditions shows much large variation at a high wind speed, corresponding to a low tip speed ratio.

This study gives an estimated level of aerodynamic damping for floating VAWTs. In the frequency-domain analysis of floating VAWTs, the aerodynamic damping should be included to provide more reasonable motion and structural responses, and give more accurate estimation of fatigue damage.

References

[1] Salzmann D J C and Tempel J V d 2005 *Proceedings of the Copenhagen Offshore Conference*
[2] Paquette J and Barone M 2012 *EWEA 2012 Annual Event*
[3] Cheng Z, Wang K, Gao Z and Moan T 2016 *Wind Energy*
[4] Antonutti R 2015 *Numerical Study of Floating Wind Turbine Hydro & Aeromechanics* PhD thesis The University of Edinburgh
[5] Cheng Z, Madsen H A, Gao Z and Moan T 2016 *Submitted to Renewable Energy*
[6] Cheng Z, Madsen H A, Gao Z and Moan T 2016 *Submitted to Renewable Energy*
[7] Robertson A, Jonkman J, Masciola M, Song H, Goupee A, Coulling A and Luan C 2012 Definition of the semi-submersible floating system for phase II of OC4 Report
[8] Jonkman J M, Butterfield S, Musial W and Scott G 2009 Definition of a 5-mw reference wind turbine for offshore system development Tech. Rep. NREL/TP-500-38060 NREL, Golden, CO, USA
[9] MARINTEK 2012 Simo-theory manual version 4.0
[10] MARINTEK 2012 Rifelx theory manual, version 4.0
[11] Madsen H A 1982 *The Actuator Cylinder: A flow model for vertical axis wind turbines* (Institute of Industrial Constructions and Energy Technology, Aalborg University Centre)
[12] Cheng Z, Madsen H A, Gao Z and Moan T 2016 *Energy Procedia (accepted)*
[13] Larsen T J and Madsen H A 2013 *Proceedings of EWEA*